Date July 2007
Author Kessel, J.L.F. van and J.A. Pinkster
Address Delft University of Technology
Ship Hydromechanics Laboratory
Mekelweg 2, 26282 CD Delft

TUDelft

Delft University of Technology

Wave-induced structural loads on different types of aircushion supported structures

by

J.L.F. van Kessel and J.A. Pinkster

Report No. 1546-P 2007

Presented at the 17th International Offshore and Polar Engineering Conference, Lisbon, Portugal 1-6 July 2007, Volume IV, ISBN 1-880653-68-0

The Proceedings of The Seventeenth (2007) International OFFSHORE AND POLAR ENGINEERING CONFERENCE

Lisbon, Portugal

VOLUME IV, 2007

FIFTH (2007) ISOPE HIGH-PERFORMANCE MATERIALS SYMPOSIUM: NANOMATERIALS FOR STRUCTURAL APPLICATION (NANOMATERIALS: APPLICATIONS, SYNTHESIS & PROCESSING, CHARACTERIZATION & MODELING)
FIRST (2007) ISOPE STRAIN-BASED DESIGN SYMPOSIUM (MATERIALS, TESTING AND EVALUATION, DESIGN AND PROJECT, MECHANICS, ASSESSMENT PROCEDURES, COMPRESSIVE STRAIN LIMIT AND BUCKLING)
HIGH-PERFORMANCE MATERIALS (ADVANCED STEEL & STRUCTURES, FATIGUE AND FRACTURE, TUBULAR STRUCTURES, ADVANCE IN WELDING TECHNOLOGY, NDE & RESIDUAL STRESS)
COMPOSITES AND SMART STRUCTURES
EARTHQUAKE AND ENGINEERING, IMPACT & COLLISION, RELIABILITY & SAFETY
SHIP STRUCTURES, ADVANCED SHIPS

How to Use This Table of Contents

Scroll down or use the bookmarks in the left-side frame to move to a new location in this index.
Click on the **blue paper title** you like to view.
To return to this index after viewing a paper, click the back button on your web browser.

This CD-ROM was created from the author-made PDF files. View quality of the text and graphics and the ease of readability depend largely on the quality and/or consistency of the PDF-making procedure the authors used.

ISBN 978-1-880653-68-5 (Vols. 1-4 Full Proceedings Set)
ISBN 1-880653-68-0 (Vols. 1-4 Full Proceedings Set)
ISSN 1098-6189 (Vols. 1-4 Full Proceedings Set)

Indexed by Engineering Index, Compendex and Others

www.isope.org

orders@isope.org

Edited by:
Hyun Woo Jin, ExxonMobil Research and Engineering Company, Annandale, New Jersey, USA
Daniel B. Lillig, ExxonMobil Development Company, Houston, Texas, USA
Thomas Tsakalakos, Rutgers University, Piscataway, New Jersey, USA
Yong-Yi Wang, Engineering Mechanics Corp., Columbus, Ohio, USA
Eiji Tsuru, Nippon Steel Co., Futtsu, Chiba-ken, Japan

Presented at:
The Seventeenth (2007) International Offshore and Polar Engineering Conference held in Lisbon, Portugal, July 1-6, 2007

Organized by:
International Society of Offshore and Polar Engineers

Sponsored by:
International Society of Offshore and Polar Engineers (ISOPE) with cooperating societies and associations

International Society of Offshore and Polar Engineers (ISOPE)
P.O. Box 189, Cupertino, California 95015-0189 USA

CONTENT

PLENARY PAPER

THE FIFTH (2007) ISOPE HIGH-PERFORMANCE MATERIALS (HPM) SYMPOSIUM: NANOMATERIALS FOR STRUCTURAL APPLICATION

NANOMATERIALS: APPLICATIONS

ADVANCED SHIPS

Wave-induced structural loads on different types of aircushion supported structures

J.L.F. van Kessel
Offshore Engineering Department, Delft University of Technology,
Delft, The Netherlands
J.A. Pinkster
Ship Hydromechanics Laboratory, Delft University of Technology,
Delft, The Netherlands

ABSTRACT

The wave-induced structural loads of different types of aircushion supported structures are described and compared with those of a rectangular barge having the same dimensions. The structural loads include the wave induced bending moments and shear forces along the length of the structure.
Aircushions can significantly influence the behaviour and structural loads of large floating structures in waves. The reduction of the bending moment shows that the use of aircushions can be of interest for large floating structures.
Calculations are based on a linear three-dimensional potential method using a linear adiabatic law to describe the air pressures inside the cushions. The water surface within the aircushions and the mean wetted surface are modelled by means of panel distributions representing oscillating sources.
Results of the calculations show that the wave-induced structural loads of aircushion supported structures are significantly smaller than those of a conventional barge, though they are not necessarily smallest in case of a large single aircushion. A structure supported by two aircushions, which provide 75% of the buoyancy, shows better results with respect to pitch motions, vertical wave shear forces and bending moments than a structure supported by one large aircushion. Furthermore, structural loads can be reduced by connecting two cushions together in a way that air can freely flow from one cushion to another.

KEY WORDS: Floating structures; aircushion support; structural loads; wave shear forces; wave bending moments; motion behaviour, Pneumatically Stabilized Platform.

INTRODUCTION

The first results on the behaviour of large aircushion supported structures in waves at Delft University of Technology were presented by Pinkster (1997). In the following years the research was continued by Pinkster, Fauzi, Inoue and Tabeta (1998) and Pinkster and Meevers Scholte (2001). Results of model tests performed by Tabeta (1998) served to validate the results of the computations. In December 2004, a PhD research started to further investigate the behaviour of Very Large Floating Structures supported by aircushions. This paper describes the Wave-induced structural loads on different types of aircushion supported structures and can be considered as an extension of the other papers written by Van Kessel and Pinkster (2007a, 2007b).

The structural loads are based on computations with the existing linear three dimensional diffraction code DELFRAC, this code was modified to take into account the effect of aircushions. The present paper describes the wave shear forces and bending moments of different configurations of aircushion supported structures at zero forward speed in waves.

Successively, the numerical approach of the computational method will be given, followed by a description of the structural loads. Finally the wave-induced structural loads on different types of aircushion supported structures will be discussed and compared with those of a conventional barge.

NUMERICAL APPROACH

The interaction between the aircushions, the structure and the surrounding water are based on a three dimensional potential theory. The rigid part of the structure is modelled in the usual way by means of panels representing pulsating sources distributed over the mean wetted surface of the construction.
The free surface within each aircushion is modelled by panels representing oscillating source distributions laying in the mean free surface of each cushion. The mean surface level of an individual cushion may be substantially different from the other cushions and the mean water level outside the structure.
All panels of the free surface within an aircushion are assumed to represent a body without material mass but having added mass, damping, hydrostatic restoring and aerostatic restoring characteristics. Use is made of a linear adiabatic law to describe the air pressures inside the cushions. The restoring coefficients as described by Van Kessel and Pinkster (2007a) are included in the numerical calculations. Each free surface panel has one degree of freedom being the vertical motion. The

total number of degrees of freedom ($D.O.F.$) therefore amounts to:

$$D.O.F. = 6 + \sum_{c=1}^{C} N_c \qquad (1)$$

in which:

N_c = number of panels in cushion c

The number 6 represents the six degrees of freedom of the rigid part of the structure. The equations of motion can in this case be written as:

$$\sum_{j=1}^{D.O.F.} \left\{ -\omega^2 \left(M_{nj} + a_{nj} \right) - i\omega b_{nj} + c_{nj} \right\} x_j = X_n, \quad n = 1, 2, ..., D.O.F. \qquad (2)$$

in which:

M_{nj} = mass coupling coefficient for the force in the n-mode due to acceleration in the j-mode. Zero for cushion panels.

a_{nj} = added mass coupling coefficient

b_{nj} = damping coupling coefficient

c_{nj} = spring coupling coefficient

x_j = mode of motion

X_n = wave force in the n-mode

The wave forces X_n, the added mass and damping coupling coefficients a_{nj} and b_{nj} are determined in the same way as is customary for a multi-body system.

The contribution of the total potential due to the discrete pulsating source distributions over the structure and the free surface of the aircushions can be expressed as:

$$\phi_j\left(\overline{X}\right) = \frac{1}{4\pi} \sum_{s=1}^{N_c} \sigma_{sj}\left(\overline{A}\right) G\left(\overline{X}, \overline{A}\right) \Delta S_s \qquad (3)$$

in which:

N_c = total number of panels of the structure and free surfaces of all cushions

$\overline{X}$ = X_1, X_2, X_3 = a field point

$\overline{A}$ = A_1, A_2, A_3 = location of a source

$G\left(\overline{X}, \overline{A}\right)$ = Green's function of a source in $\overline{A}$ relative to a field point $\overline{X}$

ΔS_s = surface element of the body or the mean free surfaces in the aircushions

σ_{sj} = strength of a source on surface element S due to motion mode j

$\phi_j\left(\overline{X}\right)$ = potential in point $\overline{X}$ due to j-mode of motion

The unknown source strengths σ_{sj} are determined based on boundary conditions placed on the normal velocity of the fluid at the centres of the panels:

$$-\frac{1}{2}\sigma_{mj}\left(\overline{X}\right) + \frac{1}{4\pi} \sum_{s=1}^{N_c} \sigma_{sj}\left(\overline{A}\right) \frac{\partial}{\partial n}\left(\overline{X}, \overline{A}\right) \Delta S_s = \frac{\partial \phi_j}{\partial n_m}, \quad m = 1, 2, ..., N_t \qquad (4)$$

STRUCTURAL LOADS

The internal shear forces and bending moments can be computed with the weight distribution of the structure and the hydrodynamic forces determined by the method as described above. In case of a rigid structure this is similar to the problem of a beam subjected to an arbitrary distributed load with additional inertia forces.

The procedure for calculation of the internal forces and moments is the same as employed in beam theory; the structure is sliced transversely at a station of interest, and a free body diagram as presented in Fig. 1 is constructed of one portion of the hull.

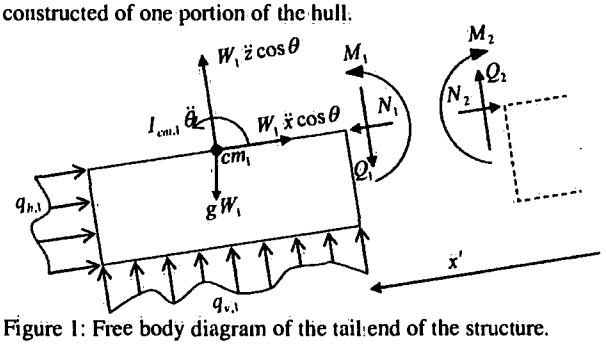

Figure 1: Free body diagram of the tail end of the structure.

A body–bound coordinate system is used with its origin connected to the centre of gravity of the floating body, in which the x-axis is positive towards the bow in longitudinal direction, the y-axis is positive towards the port side and the z-axis is directed upwards.

The shear forces and bending moments are highest when the structure is subjected to head waves. For sake of brevity shear forces and bending moments are discussed for head seas only as the effect of the aircushions will be largest in this situation. The body is considered to be rigid and the mass is equally distributed along the length of the structure.

The vertical shear force acting in the plane of a cut with a distance x' from the centre of origin can be calculated by:

$$Q_z(x') = -\int_{x'}^{\frac{L}{2}} q(x_b)\, dx_b \qquad (5)$$

in which the vertical force $q(x_b)$ along the length of the structure consists of inertia forces, hydromechanical forces and the weight of the structure. The forces on the bottom of the structure resulting from the pressures inside the aircushions are included in the hydromechanical forces. The forces acting on a segment of the structure can be written as:

$$\frac{W'}{g}\left(\ddot{z} - x_b \ddot{\theta}\right) dx_b = \left(F_z' + \rho g A_w - W'\right) dx_b + dQ_z \qquad (6)$$

in which:

W' = mass of the structure per meter

F_z' = hydromechanical forces

With use of Eq. (6), the vertical force q at a distance x_b from the centre of gravity of the structure can be written as:

$$q(x_b) = -\frac{W'}{g}\left(\ddot{z} - x_b \ddot{\theta}\right) + F_z' + \rho g A_w - W' \qquad (7)$$

The last two terms of Eq. (7) represent the static loads:

$$\rho g A_w - W' \qquad (8)$$

and the first part of Eq. (7) represents the contribution of the dynamic loads:

$$-\frac{W'}{g}\left(\ddot{z} - x_b\ddot{\theta}\right) + F_z' \tag{9}$$

Substitution of Eq. (7) in Eq. (5) results in the final expression of the vertical wave shear force at a distance x' from the centre of gravity:

$$Q_z(x') = \int_{x'}^{\frac{L}{2}} \left(\frac{W'}{g}\left(\ddot{z} - x_b\ddot{\theta}\right) - F_z' \right) dx_b \tag{10}$$

A corresponding expression of the horizontal shear force in head seas can be derived, though in this case a horizontal component of the mass-force should be added.

$$Q_x(x') = \int_{x'}^{\frac{L}{2}} \left(\frac{W'}{g}\left(\ddot{x}_b - \overline{bG}(x')\ddot{\theta}\right) - F_x' \right) dx_b \tag{11}$$

In the above, $\overline{bG}(x')$ is the vertical distance of the centre of gravity of the cross section to the body bound x-axis.

When the body is subjected to regular head seas it has an angular acceleration around this axis. The rotational equation of motion around the y-axis normal to the plane of motion can be described by an Euler equation:

$$I_{yy}\ddot{\theta} = X_{h5} + X_{w5} \tag{12}$$

in which:

X_{h5} = hydromechanical moments about the y_b-axis
X_{w5} = exciting wave moments about the y_b-axis
I_{yy} = $k_{yy}^2 m$ = mass moment of inertia around the y_b-axis
k = radius of gyration

The hydromechanical moments are induced by the harmonic oscillations of the rigid body, moving in the undisturbed surface of the fluid. The wave exciting moments are produced by waves coming in on the restrained body. Since the system is linear, the total external moment on the floating body is the sum of X_{h5} and X_{w5}.

Figure 1 shows the external forces and internal loads on a construction part at a distance x' from the centre of gravity of the total body. Here $q_{v,1}$ and $q_{v,2}$ are the external forces on the structural component, M is the bending moment, and N and Q are the horizontal and vertical shear force respectively.

The wave bending moment at a distance x' from the centre of gravity can be calculated with use of Eq. (12) and results in:

$$M(x') = I_{cm,1}\ddot{\theta} - \left(\int_{stern}^{x'} q_v(x_b)\, x_b\, dx_b + Q_1(x')\, x' \right) - \left(\int_{Dmgl} q_h(z_b)\, z_b\, dz_b + N_1(x')\,\overline{bG} \right) - g\, W_1\, \theta \tag{13}$$

in which W_1 is the weight of the structural component and $I_{cm,1}$ is the mass moment of inertia of the construction part around its centre of gravity cm_1.

Both Q and M are harmonic functions in regular waves and the amplitude depends on the wave height, as a result Eq. (10), (11) and (13) can be written as:

$$Q(x') = Q_a\, e^{i(\omega_e t + \epsilon_{Qa})} = \overline{Q_a}\, e^{i\omega_e t}$$
$$M(x') = M_{ba}\, e^{i(\omega_e t + \epsilon_{Mba})} = \overline{M_{ba}}\, e^{i\omega_e t} \tag{14}$$

It should be noted that according to Eq. (11) the vertical shear forces at the ends of the structure are equal to zero, though this is not necessarily the case for the vertical bending moments due to the presence of radiation and diffraction forces at the ends of the structure. The radiation and diffraction forces can result in horizontal shear forces at both ends of the structure as well.

WAVE-INDUCED STRUCTURAL LOADS ON AIRCUSHION SUPPORTED STRUCTURES.

The authors already showed (2007b) that a structure totally supported by a large single aircushion has the best results with respect to wave bending moments and shear forces. In case 75% of the buoyancy was provided by a large single aircushion, the maximum wave bending moment would decrease by 43% in comparison with that of a conventional barge.
A disadvantage is the relatively large pitch motion of a structure supported by a large single cushion in comparison with that of a pontoon. These large motions are caused by the lack of damping as described by the authors in (2007a).

The present paper describes the effect of aircushion division on the wave-induced structural loads. Besides, attention is paid to the pitch motions since these significantly influence the structural loads as well. The results are compared with those of a conventional barge having the same dimensions. The main particulars of all structures are:

Length	150.0	m	KG	5.0	m
Breadth	50.0	m	k_{yy}	42.0	m
Draught	5.0	m			
Displacement	38437.5	t			

The height of all cushions is 5 m and the ambient air pressure was taken equal to 100 kPa. Furthermore, the weight of the structure is equally distributed along the length of the structure and the centre of gravity is located at the centre of the structure where x = 0.

Five different aircushion configurations are compared with a conventional barge in head seas. In all cases 75% of the waterline area of the aircushion supported structures is covered by aircushions. The remaining 25% is covered by rigid skirts surrounding the cushions. The

Table 1: Cushion lengths of the aircushion configurations

Structure type / name		No. of Cushions	1st Cushion	2nd Cushion	Nth Cushion
		N x M [-]	Length [m]	Length [m]	Length [m]
1 cushion	(1AC)	1 x 1	140	-	-
2 cushions	(2AC)	2 x 1	70	70	-
2 cushions	($2AC_{angle}$)	2 x 1	70	70	-
3 cushions	(3AC)	3 x 1	30	80	30
14 cushions	(14AC)	14 x 1	2 x 5	2 x 5	2 x 5

thickness of the skirts is 5 m.

The number of cushions in lateral direction does not influence the behaviour of the structure in head seas as discussed by the authors in (2007a and 2007b). For this reason the width of all individual cushions was taken equal to 40 m. The length of the cushions of the different configurations is given in Table 1.

For sake of brevity wave forces and bending moments are discussed for head seas only as the effect of the cushions is largest in this case. The 1AC configuration is supported by a single aircushion with a length of 140 m. The 2AC configuration is supported by two cushions with a length of 70 m. The cushions of the $2AC_{angle}$ configuration are identical to the 2AC configuration, the difference is in the bow and stern of the rigid structure which are placed under an angle of 45 deg with the horizontal plane, see Fig. 2. The bow and stern of all other configurations are perpendicular to the still water line.
The 3AC configuration is supported by two cushions of 30 m at the front and back of the structure and a cushion of 80 m at the centre, see also Fig. 2.
The 14AC configuration is supported by 26 cushions with a length of 5 m and two cushions with a length of 10 m. Each cushion with a length of 5 m is connected with a second cushion as shown in Fig. 2. Air can flow freely from one cushions to another resulting in the same air pressure in both cushions.

The wetted surface of all structures, except the bow and stern of the $2AC_{angle}$ configuration, are modelled by square panels of 2.5 x 2.5 m. The length of the panels in the bow and stern of the $2AC_{angle}$ are $\sqrt{2}$ larger because these are placed under an angle of 45 degrees. The total number of panels of all other structures is equal; the rigid structure is modelled by 624 panels and the cushions by 896 panels. The total number of panels in the bottom of all structures is 1200.

The calculations of the structural loads are based on the lay-out as given in figure 3. This figure shows an aircushion configuration with N x M cushions and regular waves approaching the structure from the right side.

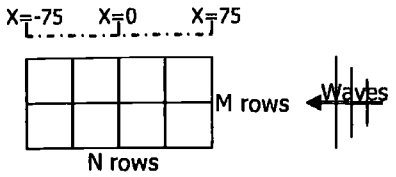

Figure 3: Lay-out of a free-floating structure supported by N x M aircushions.

Fig. 4 shows that the pitch motions of the 1AC configuration are largest, this is the result of the small pitch damping as described before. The damping of the other configurations which are supported by multiple cushions is larger, consequently the pitch motions decrease and approach those of the conventional barge.
At 0.90 rad/s the wave length is approximately equal to the length of the centre cushion of the 3AC configuration. On one hand this results in small pressure variations in the centre cushion as shown in Fig. 8. On the other hand the large air pressure variations and phase difference in the cushions at the front and back result in relatively large pitch motions at this frequency as shown in Fig. 4.
Heave motions of all aircushion configurations are approximately equal to those of the conventional barge, for this reason a figure of the heave motions is not included.

The vertical wave shear forces and bending moments of the conventional barge are presented in Fig 5. The figure shows that the shear forces are largest when the wave length is equal to the length of the structure (0.60 rad/s), in this case the maximum value is located at a distance 50 m from the centre of the structure. The smallest amplitudes of the vertical shear force are reached around the centre of gravity of the structure. A different distribution of the shear force can be seen when the length of the structure is twice the wave length (0.90 rad/s), in this case a maximum occurs at x = 0.
The right side of the structure is subjected to the incoming waves, as a result the distribution of the vertical shear forces and bending moments is not symmetrical in case the wave length is equal to the length of the structure. In this case the maximum and minimum amplitudes are shifted to the right. The wave bending moment on the other hand is largest when the wave length is approximately equal to the length of the structure at 0.60 rad/s.

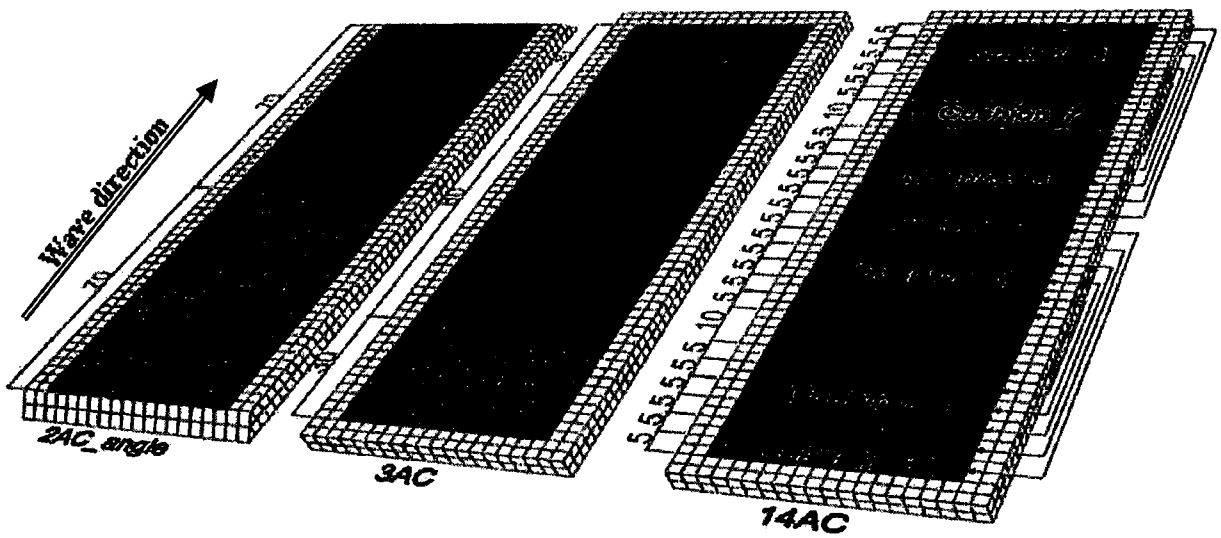

Figure 2: Panel models (of the bottom) of the $2AC_{angle}$, 3AC and 14AC configurations.

The wave shear forces and bending moments of the 1AC configuration are shown in Fig 6. The maximum wave shear force occurs at the location of the front skirt of the structure where x = 70. Moreover, the maximum value is reached when the wave length is equal to the length of the structure. The same conclusion can be drawn for the wave bending moments, though the maxima occur around the centre of the structure.
Both the vertical wave shear forces and the bending moments are significantly reduced by the aircushion. The maximum vertical wave shear force decreases by 30% in comparison with the conventional barge. The reduction of the wave bending moment is even larger and amounts to 43%.

The 2AC, 3AC and 14AC configurations are aimed at a further reduction of the wave-induced structural loads. From the previous section it becomes clear that the wave-induced internal forces and moments depend on the vertical and angular acceleration respectively. In order to reduce these accelerations, it is necessary to reduce the heave and pitch motions respectively. Since the heave motions of the aircushion supported structures and the conventional barge are approximately the same, it is difficult to reduce the vertical structural loads without applying appendages to the structure. The pitch motion on the other hand can be reduced by using multiple aircushions instead of a single large cushion as can be seen in Fig. 4.
The results of the 2AC configuration presented in Fig. 7 show a further reduction of the maximum vertical wave shear force. The maximum value occurs at the same location as was the case for the 1AC, but the force is reduced by 41% with respect to the conventional barge and 16% compared to the 1AC configuration.
The right side of the structure is subjected to the incoming waves, and consequently the air pressure variations in the front cushion (cushion 2) are larger at higher frequencies than those of the aft cushion, this can be seen in Fig. 7. The distribution of the vertical shear forces is not symmetrical at frequencies larger than 0.50 rad/s due to the difference in pressure variations and phases between the cushions.
The same figure also shows that a maximum occurs at the centre of the structure when the wave length is approximately 70 m (0.90 rad/s), this is equal to the length of the individual cushions. In this case the pressure variations in both cushions is out of phase, i.e. when the pressure increases in cushion 1 due to a wave crest, the pressure in cushion 2 decreases due to a wave through.
The maximum wave bending moment of the 2AC configuration amounts to 98% of the 1AC configuration.

Figure 8 shows the air pressure variations and the structural loads of the 3AC configuration. From this figure it becomes clear that both the wave shear forces and bending moments increase when the structure is supported by more than two aircushions in longitudinal direction. Contrary, the pitch motions decrease, but the wave bending moments increase as a result of the relatively large vertical wave loads at the ends of the structure.
The distribution of the vertical wave shear forces is not symmetrical for frequencies larger than 0.50 rad/s due to the difference in air pressure variations between the front and aft cushion.
The maximum values of the vertical wave shear forces are located at the boundaries between the cushions at x = -40 and x = 40. In comparison with the other configurations, the vertical shear force is small at the location of the skirts and the centre of the structure. The wave bending moments are larger than those of the other aircushion supported structures. The maximum wave bending moment of the 3AC configuration is 87% of that of the conventional barge.

In order to reduce the midship bending moment, the pitch motion and vertical loads at the ends of the structure should be reduced. To achieve this, the cushions at the front part of the 14AC configuration are connected with cushions in the middle, e.g. the cushion at x = 67.5 is connected with the cushion at x = 2.5. In this way the air pressure in both connected cushions is the same and the relatively high pressure in the front cushion is decreased by the low pressure in the centre cushion. The same consideration holds for the cushions in the aft portion of the construction as can be seen in Fig. 2.
Figure 9 shows the air pressure variations inside the aircushions and the distribution of structural loads of the 14AC configuration. The distribution of the vertical wave shear forces is not symmetrical around x = 0 for frequencies larger than 0.50 rad/s, this is due to the difference in air pressure variations between the cushions in the front and aft part of the construction.
The maximum vertical wave shear force and bending moment are approximately equal to those of the 1AC configuration, though they occur at different locations.
There are similarities between the 14AC configuration and the Pneumatically Stabilized Platform (PSP) as described by Blood (1996). The PSP is supported by a framework of oscillating water columns (OWCs) which are in fact small aircushions, these aircushions are linked together in a way that air can flow from one OWC to another. In case of the PSP, the airflow is also used to extracted energy from the waves which can be converted into electrical power.

An overview of the maximum amplitudes of the vertical internal loads of the aircushion configurations and the conventional barge is given in Table 2. This table clearly shows that the shear force and the bending moments of the 2AC configuration are smallest.
The maximum values of the vertical shear forces and bending moments of the $2AC_{angle}$ configuration are larger than those of the 2AC, due to the angle of the rigid skirts at the bow and stern of the structure. On the other hand, the horizontal shear forces of the $2AC_{angle}$ configuration are significantly smaller than those of the other structures as can be seen in Fig. 10.
Besides, the midship vertical shear forces and bending moments of all aircushion configurations and the conventional barge are given in Fig. 10. The figure clearly shows that aircushions can significantly reduce the vertical wave shear forces and bending moments.

Table 2: Maximum amplitudes of vertical shear forces and bending moments

	Shear Force		Bending Moment	
	[kN/m]	[-]	[kN]	[-]
1AC	3357	70%	1.19E+05	57%
2AC	2832	59%	1.17E+05	56%
$2AC_{angle}$	3172	66%	1.24E+05	59%
3AC	4340	91%	1.83E+05	87%
14AC	3175	66%	1.18E+05	56%
Barge	4783	100%	2.10E+05	100%

CONCLUSIONS

The maximum vertical wave shear forces and bending moments can be significantly reduced by the use of aircushions. A large single cushion shows good results, but the best results are obtained when the structure is supported by two aircushions in longitudinal direction. When 75% of the buoyancy is provided by two aircushions of equal size, the maximum vertical wave shear force and bending moments decrease by 41% and 44% respectively.
An additional advantage of the two cushion configuration is the reduction of the pitch motion in comparison with that of a structure supported by one large single cushion.
Contrary, the internal loads increase in comparison with the two cushion configuration when the structure is supported by more than two

cushions.

On the other hand good results with respect to vertical shear forces and bending moments can be obtained when the structure is supported by multiple cushions which are linked together in a way that air can freely flow from one cushion to another. Though this structure is more complex than a structure supported by a large single cushion, the structural loads are smaller.

Moreover, the results have shown that aircushion support can be a good solution to reduce the internal loads of large floating structures.

REFERENCES

Blood, H. (1996). "Model Tests of a Pneumatically Stabilized Platform," *Proceedings of International Workshop on Very Large Floating Platforms*, pp 77-84.

Pinkster, J.A. (1997). "The effect of air cushions under floating offshore structures," *Proceedings of Boss'97*, pp 143-158.

Pinkster, J.A., Fauzi, A., Inoue, Y. and Tabeta, S. (1998). "The behaviour of large air cushion supported structures in waves.," *Hydroelasticity in Marine Technology*, pp 497-506.

Pinkster, J.A. and Mecvers Scholte, E.J.A. (2001). "The behaviour of a large air-supported MOB at Sea," *Journal of Marine Structures*, Vol 14, pp. 163-179.

Tabeta, S. (1998). "Model experiments on barge type floating structures supported by air cushions," Report 1125, *Laboratory of Ship Hydromechanics*, Delft University of Technology, Delft.

Van Kessel, J.L.F. and Pinkster, J.A. (2007a). "The effect of aircushion division on the motions of large floating structures," *Proceedings of the 26th International Conference on Offshore Mechanics and Arctic Engineering (OMAE'07)*, ASME, No. OMAE2007-29512.

Van Kessel, J.L.F. and Pinkster, J.A. (2007b). "The effect of aircushion division on the structural loads of large floating offshore structures," *Proceedings of the 26th International Conference on Offshore Mechanics and Arctic Engineering (OMAE'07)*, ASME, No. OMAE2007-29513

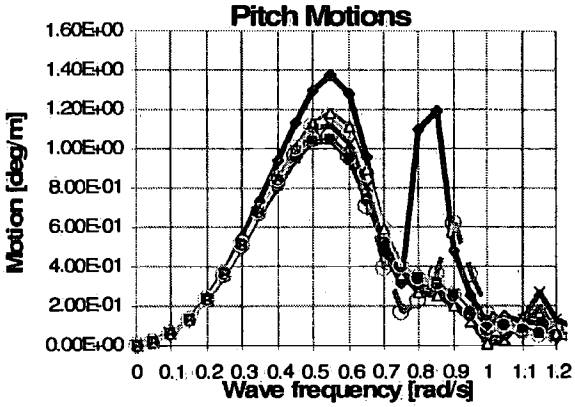

Figure 4: Pitch motions in head seas of the following structures:
Pontoon, 1AC, 2AC, 2AC_angle, 3AC, 14AC

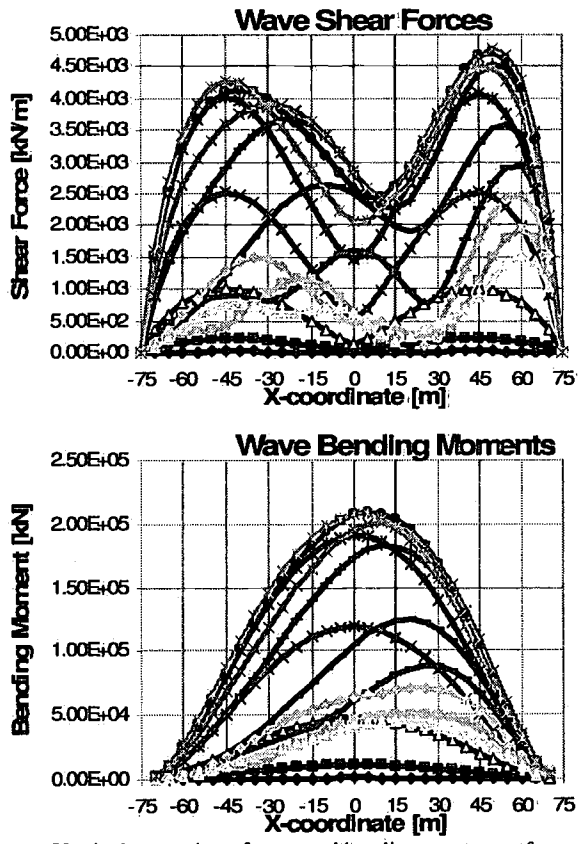

Figure 5: Vertical wave shear forces and bending momcnts of a conventional barge in head seas.

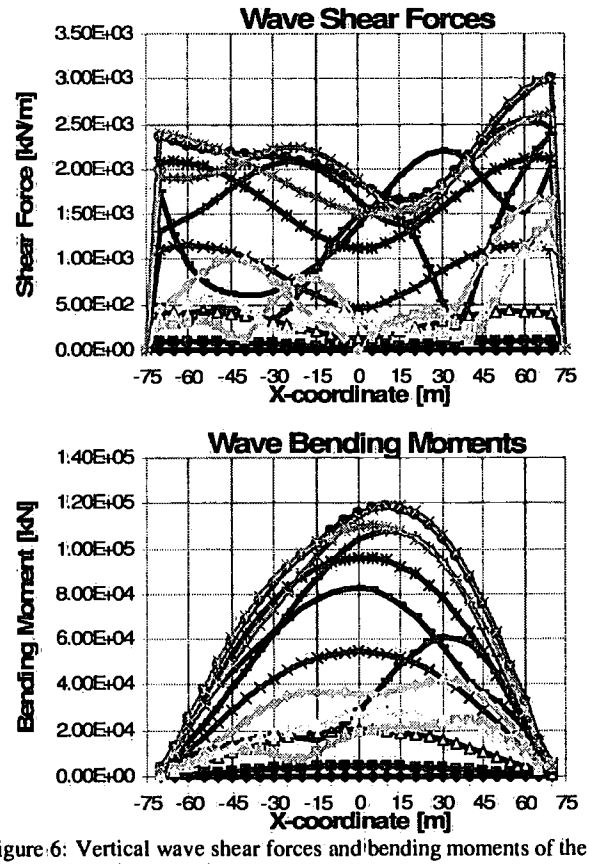

Figure 6: Vertical wave shear forces and bending moments of the 1AC configuration in head seas.

0.1 [rad/s], 0.2 [rad/s], 0.3 [rad/s], 0.4 [rad/s], 0.5 [rad/s], 0.55 [rad/s], 0.6 [rad/s], 0.65 [rad/s], 0.7 [rad/s], 0.8 [rad/s], 0.9 [rad/s], 1 [rad/s], 1.1 [rad/s], 1.2 [rad/s]

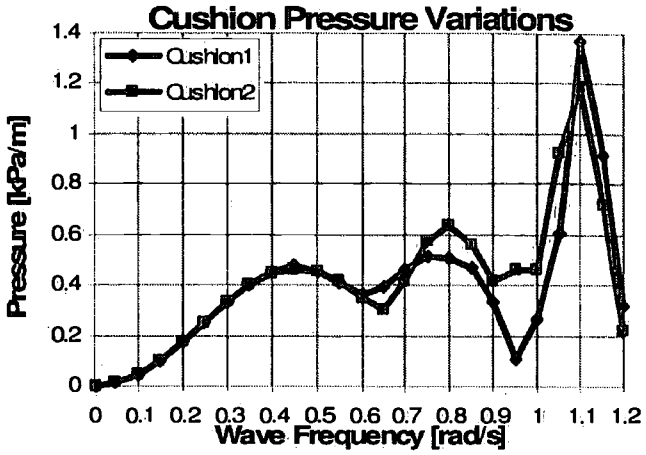

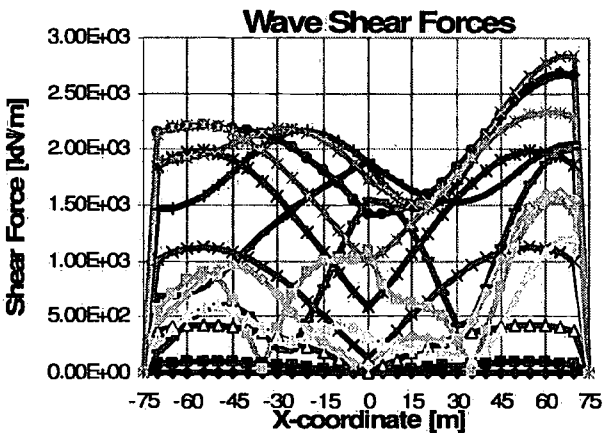

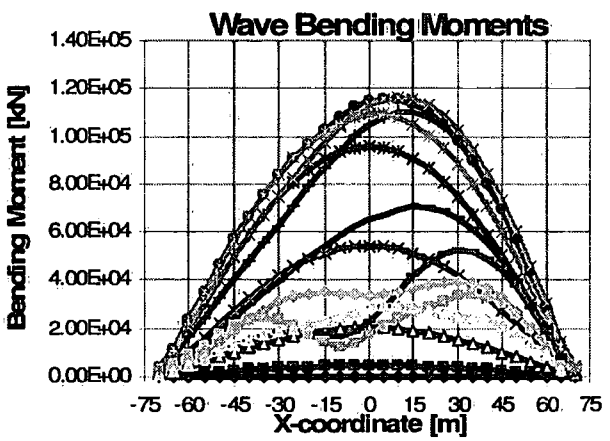

Figure 7: Air pressure variations, vertical wave shear forces and bending moments of the 2AC configuration in head seas at different wave frequencies:

0.1 [rad/s] 0.2 [rad/s] 0.3 [rad/s]
0.4 [rad/s] 0.5 [rad/s] 0.55 [rad/s]
0.6 [rad/s] 0.65 [rad/s] 0.7 [rad/s]
0.8 [rad/s] 0.9 [rad/s] 1 [rad/s]
1.1 [rad/s] 1.2 [rad/s]

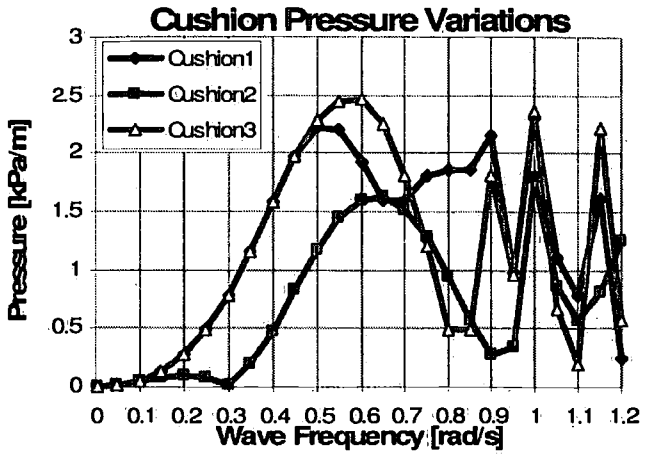

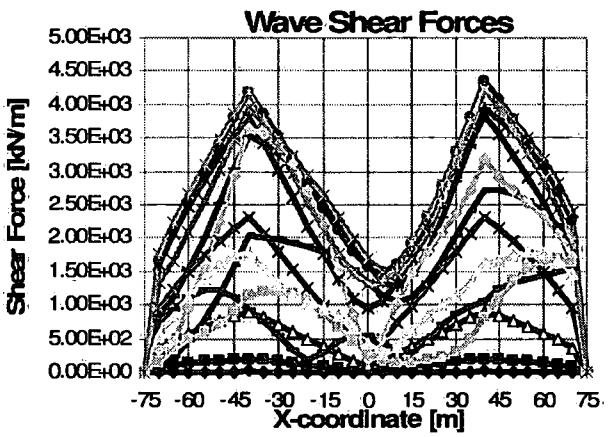

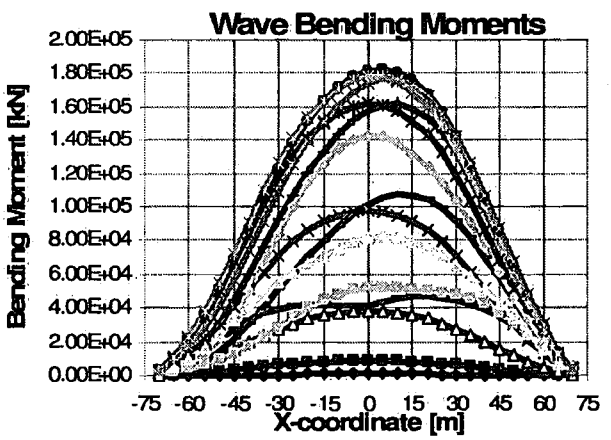

Figure 8: Air pressure variations, vertical wave shear forces and bending moments of the 3AC configuration in head seas at different wave frequencies:

0.1 [rad/s] 0.2 [rad/s] 0.3 [rad/s]
0.4 [rad/s] 0.5 [rad/s] 0.55 [rad/s]
0.6 [rad/s] 0.65 [rad/s] 0.7 [rad/s]
0.8 [rad/s] 0.9 [rad/s] 1 [rad/s]
1.1 [rad/s] 1.2 [rad/s]

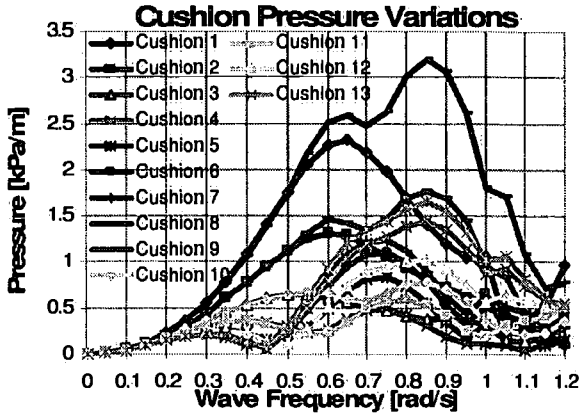

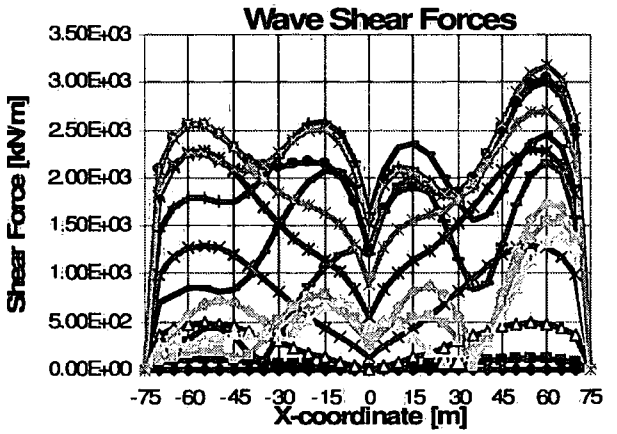

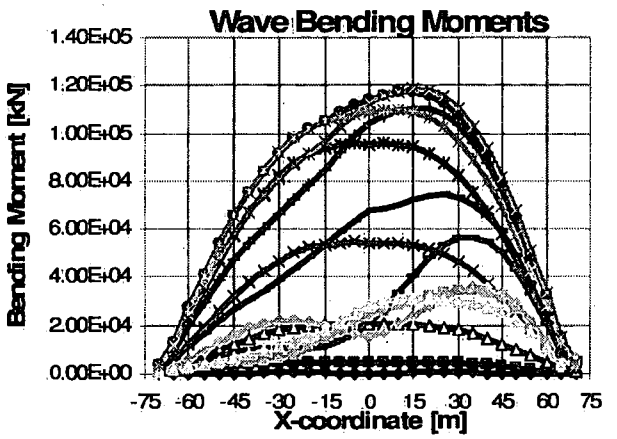

Figure 9: Air pressure variations, vertical wave shear forces and bending moments of the 14AC configuration in head seas at different wave frequencies:

0.1 [rad/s] 0.2 [rad/s] 0.3 [rad/s]
0.4 [rad/s] 0.5 [rad/s] 0.55 [rad/s]
0.6 [rad/s] 0.65 [rad/s] 0.7 [rad/s]
0.8 [rad/s] 0.9 [rad/s] 1 [rad/s]
1.1 [rad/s] 1.2 [rad/s]

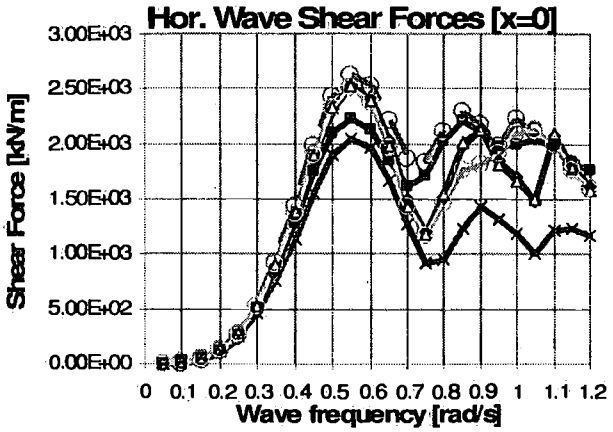

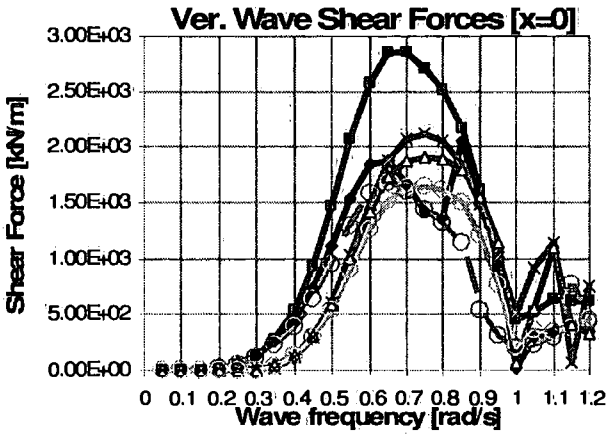

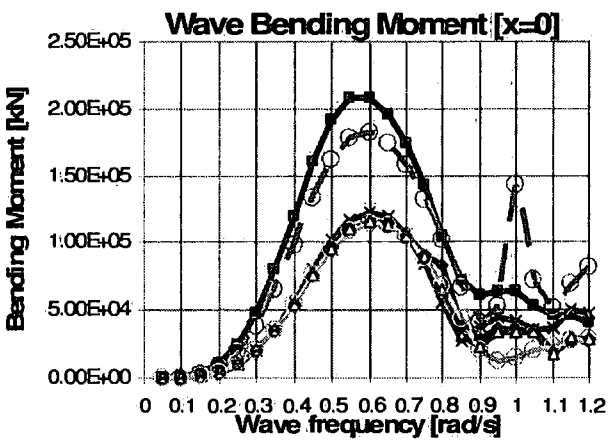

Figure 10: Amplitudes of the horizontal wave shear forces, vertical wave shear forces and wave bending moments of all structures in head seas.

Pontoon 1AC 2AC
2AC_angle 3AC 14AC